RESEARCH ARTICLE

The non-glycosylated protein of *Toxocara canis* MUC-1 interacts with proteins of murine macrophages

Rongqiong Zhou[1,2], Hongguo Jia[1], Zhendong Du[3], Aiyun Jiang[1], Zhenhui Song[1], Tao Wang[4], Aifang Du[3], Robin B. Gasser[4]*, Guangxu Ma[3,4]*

1 College of Veterinary Medicine, Southwest University, Chongqing, China, **2** Immunology Research Center, Medical Research Institute, Southwest University, Chongqing, China, **3** Institute of Preventive Veterinary Medicine, Zhejiang Provincial Key Laboratory of Preventive Veterinary Medicine, College of Animal Sciences, Zhejiang University, Hangzhou, China, **4** Department of Veterinary Biosciences, Melbourne Veterinary School, The University of Melbourne, Parkville, Victoria, Australia

* robinbg@unimelb.edu.au (RBG); gxma1@zju.edu.cn (GM)

Abstract

Toxocariasis is a neglected parasitic disease caused predominantly by larvae of *Toxocara canis*. While this zoonotic disease is of major importance in humans and canids, it can also affect a range of other mammalian hosts. It is known that mucins secreted by larvae play key roles in immune recognition and evasion, but very little is understood about the molecular interactions between host cells and *T. canis*. Here, using an integrative approach (affinity pull-down, mass spectrometry, co-immunoprecipitation and bioinformatics), we identified 219 proteins expressed by a murine macrophage cell line (RAW264.7) that interact with pro-karyotically-expressed recombinant protein (r*Tc*-MUC-1) representing the mucin *Tc*-MUC-1 present in the surface coat of infective larvae of *T. canis*. Protein-protein interactions between r*Tc*-MUC-1 and an actin binding protein CFL1 as well as the fatty acid binding protein FABP5 of RAW264.7 macrophages were also demonstrated in a human embryonic kidney cell line (HEK 293T). By combing predicted structural information on the protein-protein interaction and functional knowledge of the related protein association networks, we inferred roles for *Tc*-MUC-1 protein in the regulation of actin cytoskeletal remodelling, and the migration and phagosome formation of macrophage cells. These molecular interactions now require verification *in vivo*. The experimental approach taken here should be readily applicable to comparative studies of other ascaridoid nematodes (e.g. *T. cati*, *Anisakis simplex*, *Ascaris suum* and *Baylisascaris procyonis*) whose larvae undergo tissue migration in accidental hosts, including humans.

Author summary

Toxocariasis is a neglected parasitic disease of humans caused mainly by larvae of *Toxocara canis*. Given that *T. canis* is zoonotic and can infect a range of mammals, there has been substantial interest in host-parasite relationships, with studies showing that *T. canis*

larvae secrete abundant mucins that effect/modulate immune responses and disease pathogenesis. To improve the understanding of immunomolecular interactions, we investigated the role(s) of the protein component of a mucin (*Tc*-MUC-1) secreted by infective larvae using a well-defined murine macrophage line (RAW264.7). The non-glycosylated recombinant protein of *Tc*-MUC-1 (designated r*Tc*-MUC-1) was shown to interact with at least 219 proteins of RAW264.7 cells, particularly with the actin binding protein (CFL1) and a fatty acid binding protein (FABP5), which are involved in cell migration and phagocytosis, respectively. Based on these findings, we propose that *Tc*-MUC-1 regulates cytoskeletal organisation and signal transduction in host macrophages. It would be interesting to establish, using the integrative experimental approach employed here, whether the role(s) of *Tc*-MUC-1 protein homologues of related ascaridoids are conserved.

Introduction

Human toxocariasis is a neglected parasitic disease of global importance [1]. It is caused by the larvae of *Toxocara* species, usually transmitted from domestic and stray canids or felids to humans and other mammals via the ingestion of infective eggs from the contaminated environment, food or water, or via infective larvae in undercooked meat [2,3]. Although most people infected with *Toxocara* larvae are asymptomatic, it has been estimated that ~ 1.4 billion people worldwide are exposed to, or infected with, *T. canis* and *T. cati*, particularly young children and pet owners [4,5]. The four main forms of human toxocariasis include visceral larva migrans (VLM), ocular larva migrans (OLM), neurotoxocariasis (NT) and covert/common toxocariasis (CT), and there is evidence of associations between anti-*Toxocara* seropositivity and asthma, idiopathic Parkinson's disease and Alzheimer's disease in humans [6–11]. Most anthelmintic drugs are not effective against larvae in tissues of the human host, and no vaccine is available for the prevention of human toxocariasis.

Apart from humans, eggs containing larvae of *Toxocara* species can infect many mammalian species as paratenic or accidental hosts; in these hosts, larvae that emerge from the eggs in the host gut migrate to various tissues and cause infection or toxocariasis but do not develop to adults in the small intestine [2]. Fundamental investigations of human toxocariasis have relied heavily on the use of rodent (mouse, rat and jird) models [12,13]. The mouse model has been particularly useful to study host-parasite interactions, including the immunobiology of *Toxocara*/toxocariasis [14]. Clearly, a sound understanding of such interactions in the mouse model at the immunomolecular level is key to underpinning toxocariasis research and to developing new interventions.

Over the past seven decades [15,16], our understanding of the immunobiology of *Toxocara* has improved significantly [17–19]. For example, a series of molecules likely associated with *Toxocara* development, infection and parasitism have been discovered by informatic analyses of genomic, transcriptomic and proteomic data sets [20–26] and explored *in vitro* and *in vivo* [20]. Importantly, lectins (also known as TES-32 and -70) and mucins (also known as TES-120) excreted/secreted by *Toxocara* have been inferred to play crucial roles in the escape of larvae from surrounding cells and ensuing tissue inflammation within host animals [20–22]. Specifically, mucins of *T. canis* (i.e. *Tc*-MUC-2, -3, -4 and -5) have been reported to induce the secretion of cytokines by mouse splenocytes and to modulate the Toll-like receptor signalling in human THP-1 macrophages, indicating an involvement in the host-parasite interplay [23,24]. However, apart from mainly serological investigations [25–28], little is known about the molecular processes/mechanisms underlying the interactions between *Toxocara* mucins

and host immune cells, particularly at a protein-protein level. In order to gain a better understanding of these aspects, we investigated proteins of murine macrophage cells that interact with a recombinant (non-glycosylated) form of *Tc*-MUC-1 (designated r*Tc*-MUC-1) using a pull-down assay coupled to liquid chromatography-tandem mass spectrometry (LC-MS/MS), explored key protein-protein interactions by co-immunoprecipitation, and inferred structural and functional roles of the *Tc*-MUC-1 protein in host-parasite interactions.

Methods

Ethics statement

Adult worms of *T. canis* were collected from dogs with naturally acquired infection in the Animal Hospital affiliated to the College of Animal Sciences. Collection and experimentation were approved (permit no. 20170177) by the Ethics Committee of Zhejiang University, Hangzhou, China.

Worms and cell lines

Eggs were collected from the uteri of adult females of *T. canis*, incubated in H_2O for 8 weeks at 25˚C and manually hatched with glass beads. The third-stage larvae (L3s) of *T. canis* released from the eggs were purified and enriched using the Baermann method [29], snap frozen in liquid nitrogen and stored in -80˚C until use. Murine macrophage cells (RAW264.7) and human embryonic kidney cells (HEK 293T) were purchased from Beyotime Biotechnology, Shanghai, and maintained according to the manufacturer's instructions.

RNA extraction and cDNA synthesis

Total RNA was extracted from pooled *T. canis* L3s (n = 3000) using Trizol reagent (Ambion, Thermo Fisher Scientific). RNA was reverse-transcribed into the first-strand cDNA using a PrimeScript RT Reagent Kit (Takara Bio, Dalian), according to the manufacturer's protocol. The synthesised cDNA was stored at -20˚C until use.

Molecular cloning of *Tc-muc-1*

Using the program Primer Premier 5.0 (Premier Biosoft International, Palo Alto, CA), primers (forward: 5´-ATGCACGTCCTTACCGT-3´; reverse: 5´-TTAACAGAAGCCGCACGT-3´) were designed specifically to the mRNA sequence encoding the surface coat glycoprotein TES-120 precursor (*nmuc-1*) of *T. canis* (GenBank accession number U39815.1; ref. [30]). Synthesised cDNA template was amplified by PCR in standard buffer containing forward primer and reverse primers (10 pmol/μL each), 2.5 mmol/L Mg^{2+}, 2.5 mmol/L of each dNTP and 0.25 U rTaq polymerase (Takara Bio, Dalian) using the following profile: 94˚C for 3 min (denaturation), 35 cycles of 94˚C for 30 s (denaturation), 55˚C for 30 s (annealing) and 72˚C for 1 min (extension), then 72˚C for 5 min (final extension). PCR products were examined by agarose gel (1.0%) electrophoresis, purified, cloned into the pMD19-T (simple) vector (Takara Bio, Dalian), and competent DH5α *Escherichia coli* (TransGen Biotech, Beijing) transformed. Clones with inserts (n = 3) were selected and insert sequences confirmed by nucleotide acid sequencing (Sangon Biotech, Shanghai). The sequences were compared with those in the NCBI database nucleotide collection (nr/nt) by BLASTn (https://blast.ncbi.nlm.nih.gov/Blast.cgi) and those in SMART, Pfam and signal peptide databases using HMMER [31].

Prokaryotic expression of r*Tc*-MUC-1

A recombinant form of the *T. canis* mucin 1 protein (r*Tc*-MUC-1) fused to a 6× His tag was produced in a prokaryotic expression system. In brief, the *Tc-muc-1* protein-coding sequence was amplified with a primer set containing *Kpn* I and *EcoR* I restriction sites (5'-GGGGTACC ATGCACGTCCTTA-3'; 5'-GGAATTCTTAACAGAAGCCGCACGT-3'), and inserted into the pCold TF plasmid (Takara Bio, Dalian) employing the *Kpn* I and *EcoR* I restriction sites. Recombinant plasmids were purified, verified by specific PCR-amplification and competent BL21 (DE3) *E. coli* (TransGen Biotech, Beijing) transformed. Following induction with 0.6 mM isopropyl β-d-1-thiogalactopyranoside (IPTG), r*Tc*-MUC-1 was expressed in a culture volume of 250 ml at 37°C for 24 h. Proteins were released from cells by sonication (1 s–on, 3 s–off for 15 min on ice) at 400 W using a Scientz-IID ultrasonic homogenizer (Scientz, China). The sonicates (25 ml each) were centrifuged at 14,000 × g and 4°C for 20 min, and supernatants filtered (0.22 μm aperture) and run through a Ni-NTA column (Sangon Biotech, Shanghai); r*Tc*-MUC-1 was eluted from the column with 250 mM imidazole and subjected to SDS-PAGE analysis using an established protocol [32]. *E. coli* transformed with the pCold TF empty plasmid was used as a negative control throughout experimentation.

Pull-down assay

The RAW264.7 macrophage cell line was cultured in 2 ml Dulbecco's modification of Eagle Medium (DMEM; Thermo Fisher Scientific) supplemented with 10% (v/v) foetal bovine serum, 100 IU/mL of penicillin, 100 μg/mL of streptomycin and 2.5 μg/mL of amphotericin (Antibiotic–Antimycotic, Thermo Fisher Scientific) and 1% L-glutamine at 37°C and 5% CO_2. When a confluence of 80% was reached, proteins were extracted from the culture (six wells) by washing RAW264.7 cells twice in phosphate-buffered saline (PBS, pH 7.5), incubation in 1.8 ml non-denaturing lysis buffer (Thermo Fisher Scientific) supplemented with 1 mM phenyl-methanesulfonyl fluoride (PMSF; Thermo Fisher Scientific) on ice for 30 min, and centrifugation at 14000 × g (4°C) for 5 min.

A poly-His affinity pull-down method [33] was used to isolate proteins in RAW264.7 macrophage cells that bind r*Tc*-MUC-1. *E. coli* expressing r*Tc*-MUC-1 was used to produce the bait protein, which was immobilised on a Ni-NTA column (Sangon Biotech, Shanghai) and washed three times with 2 mL of 10 mM imidazole. The immobilised bait protein was incubated with 1 mL of protein extract from RAW264.7, incubated at 4°C for 4 h and washed three times with 2 mL of 10 mM imidazole. Bait and target proteins were eluted (three times) from the column with 250 mM imidazole. The His-tagged protein expressed by *E. coli* containing the empty pCold TF plasmid vector was used as a negative control. Eluted proteins were resolved by SDS-PAGE and stained with silver (Silver Stain for Mass Spectrometry kit, Pierce, Thermo Fisher Scientific).

LC-MS/MS

An in-gel digestion approach was employed to process the proteins from SDS-PAGE gels. In brief, band slices were reduced with 10 mM (2S,3S)-1,4-bis-sulfanylbutane-2,3-diol, alkylated with 55 mM iodoacetamide and digested with 1 μg trypsin (Pierce, Thermo Fisher Scientific) at 37°C overnight. Peptide desalting was performed using a C18 resin column (Pierce, Thermo Fisher Scientific). Desalted peptides were freeze-dried, resuspended in 15 μL aqueous 3% w/v acetonitrile and 0.1% v/v formic acid, and then subjected to LC-MS/MS using the ekspertTM-nanoLC and AB TripleTOF 5600-plus (SCIEX) via a service provider (GeneCreate Biological Engineering Co., Ltd., Wuhan, China). Proteomic data (identifier PXD030007) have been deposited into the PRIDE partner repository of the ProteomeXchange Consortium [34].

Raw mass data were processed using ProteinPilot software (SCIEX) using five search parameters (enzyme of trypsin, Cys alkylation of iodoacetamide, bias correction of true, background correction of true, protein mass of unrestricted) against the *Mus musculus* proteome in the UniProt database. Peptide identification was performed with a confidence of $\geq$ 95%. Common contaminants (including keratin, antibodies and serum albumin or globulins) were filtered-out prior to the identification of proteins that bind r*Tc*-MUC-1. Identified proteins were annotated based on the UniProt database and Gene Ontology (GO) resources using the OmicsBean data integration analysis platform, and based on the Kyoto Encyclopedia of Genes and Genomes database using the KEGG Orthology-Based Annotation System (KOBAS 3.0) [35]. Protein network analysis was performed using STRING 10.0 software and displayed using Cytoscape 3.4.0 platform [36,37].

Eukaryotic expression

The protein-coding sequence of *Tc-muc-1* was amplified with primers 5'-CGGGATTCATGC ACGTCCTTA-3' (*Bam*H I restriction site underlined) and 5'-GGAATTCTTAACAGAAGC CGCACGT-3' (*Eco*R I restriction site underlined), and then inserted into the pcDNA3.1-Flag vector, in order to express a FLAG-tagged *Tc*-MUC-1 fusion protein. HEK 293T cells containing plasmids expressing selected His pull-down proteins of RAW264.7 macrophage cells were prepared. In brief, coding sequences were PCR-amplified using the *Eco*R I- and *Bgl* II-site containing primers (S1 Table), and then inserted into the pCMV-HA vector to produce haemagglutinin (HA)-tagged fusion proteins. Recombinant plasmids were purified using the Qiagen Ultrapure 100 system. HEK 293T cells were transfected with recombinant endotoxin-free plasmids (5 μg) using the ExFect 2000 Transfection Reagent (Vazyme), and cultured in DMEM at 37˚C and 5% CO_2. The culture medium was exchanged with DMEM supplemented with 10% v/v foetal bovine serum 12 h after transfection, and incubated at 37˚C and 5% CO_2 for 36 h.

Co-IP

The Co-IP assay was employed to confirm the interaction between r*Tc*-MUC-1 and individual partner proteins from RAW264.7 macrophage cells. To extract total proteins, cells transfected with recombinant plasmids were washed with PBS (pH 7.5), suspended in 20 μL NP40 lysis buffer (Beyotime Biotechnology, Shanghai) with 1 mM phenylmethylsulfonyl fluoride (PMSF) on ice for 30 min, and then centrifuged at $14,000 \times g$ (4˚C) for 15 min. Protein A superparamagnetic beads (Dynabeads, Thermo Fisher Scientific) were washed twice in PBS (pH 7.5), and then incubated with 3 μL mouse DYKDDDK tag monoclonal antibody (binds to FLAG tag epitope; α-Flag) (Proteintec, Wuhan). Pre-immune serum IgG was used as the negative control. Processed beads were incubated with proteins (50 μL) extracted from HEK 293T cells at 4˚C for 4 h, washed three times with PBS (pH 7.5), and mixed with 20 μL PMSF-containing NP40 lysis buffer and 5 μL loading buffer (1.5% Tris, 9.4% glycine and 0.5% SDS, pH 8.3). Protein samples were then boiled for 10 min, separated from the beads and transferred to new tubes.

Immunoblot analysis

Individual protein samples were subjected to SDS-PAGE analysis, transferred to a polyvinylidene fluoride (PVDF) membrane (Roche), and blocked with freshly prepared blocking reagent (i.e. Tris-HCl buffer, pH 8.0, containing 0.05% Tween 20 and 3% skim milk) at 4˚C for 12 h. Blocked membranes were incubated in 1:10,000 diluted mouse anti-FLAG tag monoclonal antibody or rabbit anti-HA tag polyclonal antibodies (α-HA; Proteintec, Wuhan) at 23˚C for 1.5 h, and then washed five times with Tris-HCl buffer (pH 8.0) containing 0.08% NaCl and

0.05% Tween 20 (TBST). Subsequently, the membrane was incubated with HRP-conjugated affinity-purified goat-anti rabbit IgG (1: 10,000) at 23°C for 1 h, washed five times in TBST and reacted with 3,3′-diaminodbenzidine (Pierce, Thermo Fisher Scientific) to detect proteins.

Structural modelling and docking

The three-dimensional structures of non-glycosylated *Tc*-MUC-1 (without a signal peptide) and its interacting proteins were modelled using the programs I-TASSER [38–40] and Alpha-Fold2 [41], and GO annotations predicted. *In silico* protein-protein docking was performed using the ClusPro server [42,43] based on resolved/modelled structures [44]. Protein complexes were analysed and displayed using the PyMOL molecular graphics system v2.5 (Schrö-dinger, LLC), and predicted binding sites in the *Tc*-MUC-1 and protein networks in murine macrophages.

Results

Tc-MUC-1 is predicted to have protein binding activity

A complete cDNA sequence, called *Tc-muc-1* (531 nt in length), encoding the surface coat gly-coprotein TES-120 precursor (*nmuc-1*) of infective larvae of *T. canis* (Fig 1A) was obtained. From this sequence, an amino acid sequence of 176 aa in length was deduced (called *Tc*-MUC-1) that contained a signal peptide, a low complexity region with STSSSS(P)A repeats, and two ShKT (also known as nematode six-cysteine domain or ion channel regulator) domains (Fig 1B). A U-shaped structure of *Tc*-MUC-1 was modelled, with two ShKT domains folded in the centre (Fig 1C). The fold of each ShKT domain contained two nearly perpendicular stretches of helices, stabilised by three disulfide bridges (Fig 1C). With reference to the functional infor-mation in the PDB database, ShKT domain-containing *Tc*-MUC-1 was predicted to have a binding activity (GO:0005488), particularly protein binding (GO:0005515) and metal ion
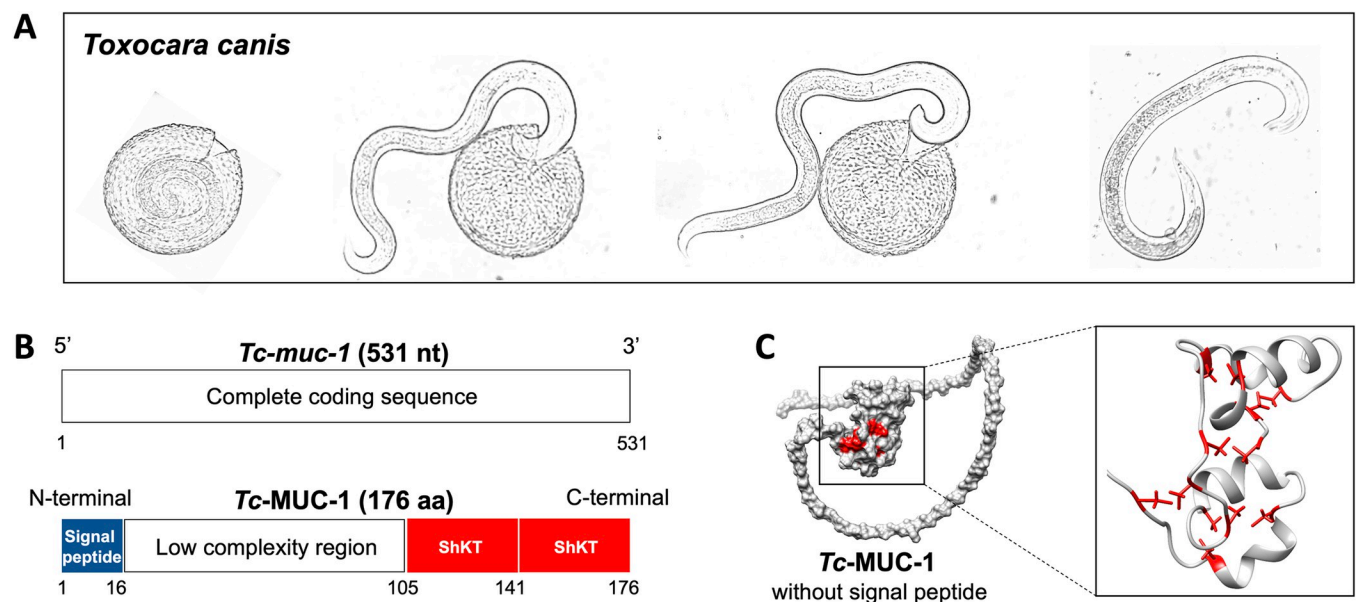
Fig 1. Molecular cloning and functional prediction of *Toxocara canis* mucin 1 (*Tc*-MUC-1). (**A**) Infective larvae of *T. canis* hatch from eggs *in vitro* are used for the molecular cloning of the gene (*Tc-muc-1*) encoding the *Tc*-MUC-1 protein. (**B**) Schematic diagram of *Tc-muc-1* and the predicted domain architecture of *Tc*-MUC-1. Signal peptide, low complexity region and two abutting ShKT domains are indicated. (**C**) The three-dimensional structure of *Tc*-MUC-1 (without signal peptide) modelled using AlphaFold2 [38]. Cysteine residues and disulfide bonds in each ShKT domain are indicated in red.

https://doi.org/10.1371/journal.pntd.0010734.g001

binding (GO:0046872). No specific binding site was predicted with confidence, due to limited structural and functional information on mucins of *T. canis* and related parasitic worms.

The r*Tc*-MUC-1 protein interacts with at least 219 proteins of murine macrophages

To understand aspects of the host-parasite interplay at the protein-protein level, molecules in murine RAW264.7 macrophage cells that directly or indirectly bound r*Tc*-MUC-1 of *T. canis* were analysed using His pull-down and subsequent mass spectrometry (Fig 2A–2D). A total of 618 peptides representing 219 proteins were identified by LC-MS/MS, 109 proteins for which at least two unique peptides (S2 and S3 Tables) were detected. Apart from 31 presently uncharacterised molecules, the other proteins identified (*n* = 188) were comprehensively annotated with Gene Ontology (GO) terms and/or linked to Kyoto Encyclopedia of Genes and Genomes (KEGG) pathways. The annotated proteins, predominantly associated with extracellular region and exosome, were functionally enriched in terms of RNA, protein, lipid and/or substrate binding, and are suggested to play roles in organonitrogen compound metabolism and biosynthetic processes (Figs 2D and S1 and S4 Table). These proteins appear to be involved particularly in multiple pathways, including metabolism, genetic information processing (e.g. protein processing in endoplasmic reticulum and RNA degradation), cellular processes (transport and catabolism, cellular community) and organismal systems (e.g. peroxisome, antigen processing and presentation pathway and nucleotide binding oligomerization domain (NOD)-like
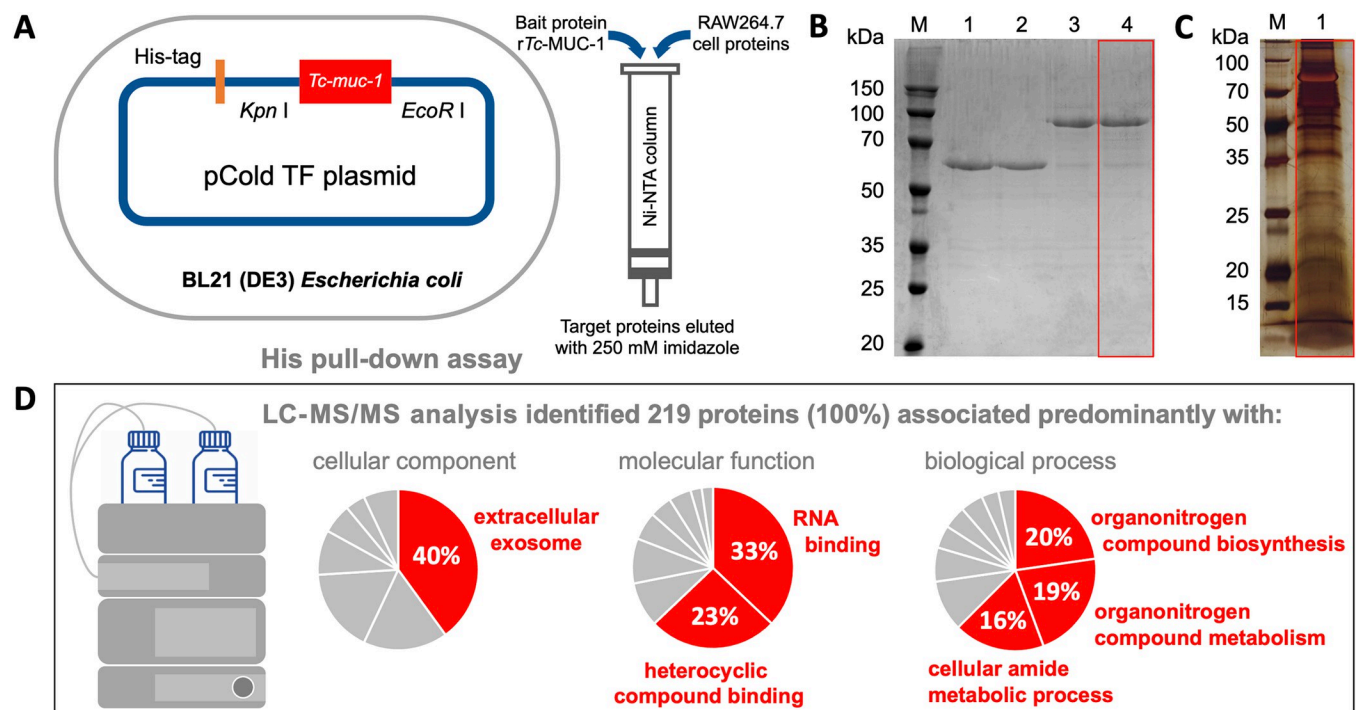

Fig 2. Pull-down and mass spectrometric analyses to identify proteins in murine macrophages that bind recombinant *Toxocara canis* mucin 1 (r*Tc*-MUC-1). (**A**) Prokaryotic expression of His-tagged bait protein (r*Tc*-MUC-1) and elution of proteins of RAW264.7 macrophages bound to a Ni-NTA column. (**B**) SDS-PAGE analysis of r*Tc*-MUC-1 and proteins pulled down by r*Tc*-MUC-1. M: protein marker; Lane 1: Empty His-tag peptide (~ 55 kDa); Lane 2: proteins of RAW264.7 cells targeted by the empty His-tag peptide; Lane 3: purified r*Tc*-MUC-1 fused to His-tag peptide (~ 75 kDa); Lane 4: proteins of RAW264.7 cells targeted by purified His-tag fused *rTc*-MUC-1 (red box indicated). (**C**) Proteins of RAW264.7 cells pulled down by r*Tc*-MUC-1, and resolved by SDS-PAGE and stained with silver stain (red box indicated). (**D**) LC-MS/MS analysis of proteins pulled down by r*Tc*-MUC-1. Peptides and proteins identified as well as the predominant functional predictions (cellular component, molecular function and biological processes) are indicated.

receptor signalling pathway) (S2 Fig and S5 Table). Based on information available for functional protein associations in the mouse, a complicated protein-protein interaction network was predicted for 147 of the mouse proteins identified (S3 Fig and S6 Table).

The r*Tc*-MUC-1 protein binds a cofilin and a fatty acid binding protein of murine macrophages

The protein-protein interactions for selected molecules with enriched extracellular and functional annotations (S3 and S4 Tables) were examined in a human embryonic kidney cell line (HEK 293T). Selected candidates included aldo_ket_red domain-containing protein (AKR1B3; UniProt accession no. Q3UDY1), rho GDP-dissociation inhibitor 1 (ARHGDIA; UniProt accession no. Q99PT1), cofilin 1 (CFL1; UniProt accession no. Q544Y7), fatty acid binding protein 5 (FABP5; UniProt accession no. Q05816), peroxiredoxin 1 (PRDX1; UniProt accession no. P35700) and profilin (PFN1; UniProt accession no. Q8CEH8) of RAW264.7 cells (Unused score > 8; *P* value < 1.00E-40) (Fig 3A). HA-tagged candidates AKR1B3, ARHGDIA, CFL1, FABP5, PRDX1 and PFN1 as well as FLAG-tagged r*Tc*-MUC-1 were successfully expressed in HEK 293T cells, and identified by respective α-HA antibodies and α-FLAG antibodies (Fig 3B–3G). We found that only CFL1, FABP5, and potentially PFN1, of RAW264.7 murine macrophages were immunoprecipitated by r*Tc*-MUC-1 and recognised by both α-HA and α-FLAG antibodies (Fig 3E and 3F). No co-immunoprecipitation of r*Tc*-MUC-1 and recombinant AKR1B3, ARHGDIA or PRDX1 was evident (Fig 3C, 3D, 3G and 3H).
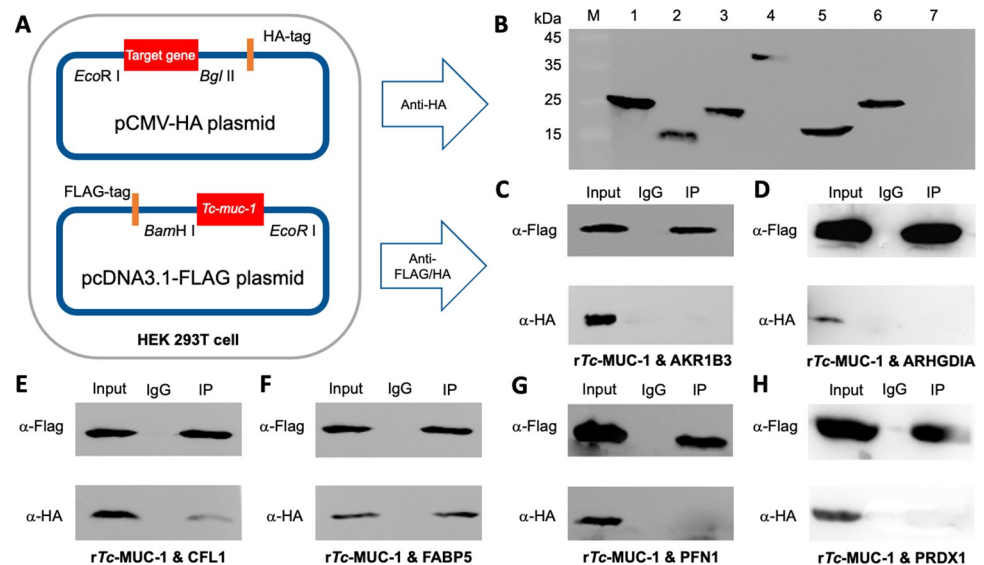
Fig 3. Co-immunoprecipitation analysis of proteins of murine macrophages bound to recombinant *Toxocara canis* mucin 1 (r*Tc*-MUC-1). (**A**) Eukaryotic expression of FLAG-tagged *Tc*-MUC-1 of *T. canis* and HA-tagged aldo_ket_red domain-containing protein (AKR1B3), rho GDP-dissociation inhibitor 1 (ARHGDIA), cofilin 1 (CFL1), fatty acid binding protein 5 (FABP5), peroxiredoxin 1 (PRDX1) and profilin (PFN1) of murine RAW264.7 macrophages in HEK 293T cells. (**B**) Western blot analyses of the expression of HA-tagged PRDX1 (lane 1), PFN1 (lane 2), CFL1 (lane 3), AKR1B3 (lane 4), FABP5 (lane 5), ARHGDIA (lane 6) and FLAG-tagged *Tc*-MUC-1 in transfected HEK 293T cells, using anti-haemagglutinin (HA)-tagged tag polyclonal antibodies (α-HA). M: Maker. Uncropped blot image can be found in S4 Fig. Western blot analyses of the expression of *Tc*-MUC-1, and (**C**) AKR1B3, (**D**) ARHGDIA, (**E**) CFL1, (**F**) FABP5, (**G**) PRDX1, and (**H**) PFN1 in transfected HEK 293T cells (Input), and in immunoprecipitated complex (IPC), using DYKDDDK tag monoclonal antibody (binds to FLAG tag epitope (α-Flag). Mouse IgG was used as a blank control.
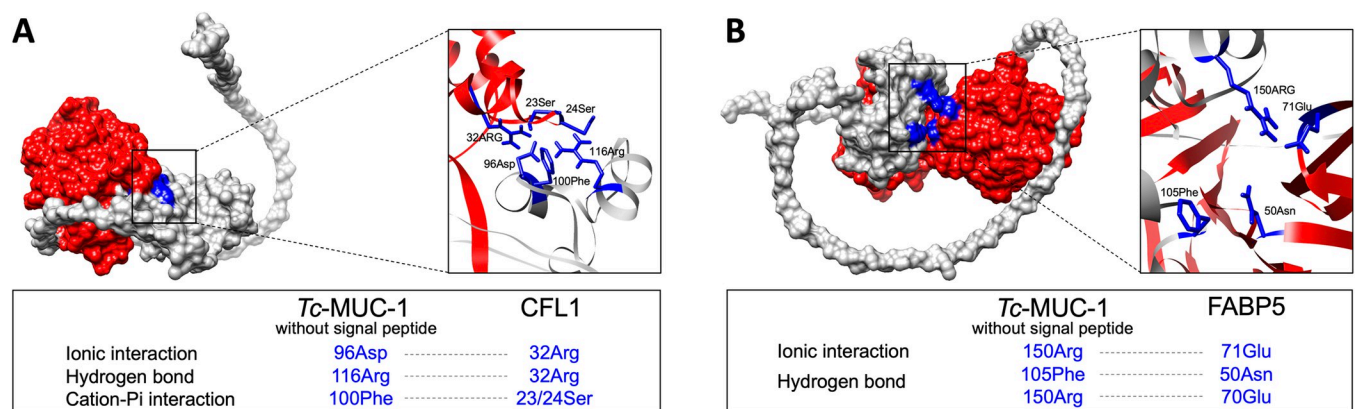
https://doi.org/10.1371/journal.pntd.0010734.g003

Protein complexes with the r*Tc*-MUC-1 protein indicate non-covalent interactions

Based on the experimentally confirmed physical interactions of r*Tc*-MUC-1 with CFL1 and FABP5, the corresponding protein complexes *Tc*-MUC-1–CFL1 and *Tc*-MUC-1–FABP5 were modelled (Fig 4). *Tc*-MUC-1–CFL1 was predicted to be stabilised by ionic interaction (between 96Asp in *Tc*-MUC-1 and 32Arg in CFL1), hydrogen bonds (between 116Arg in *Tc*-MUC-1 and 23/24Ser in CFL1), and cation-Pi binding interaction (between 100Phe in *Tc*-MUC-1 and 32Arg in CFL1) (Fig 4A). *Tc*-MUC-1–FABP5 was predicted to be stabilised by ionic interaction (between 150Arg in *Tc*-MUC-1 and 71Glu in FABP5) and hydrogen bonds (between 105 Phe and 150Arg in *Tc*-MUC-1 and 50Asn and 70Glu in FABP5) (Fig 4B). Although these protein-protein interactions were both non-covalent, different residues in *Tc*-MUC-1 are proposed to be involved and to bind multiple proteins.

Interactions suggest that the *Tc*-MUC-1 protein is linked to cytoskeletal dynamics and signalling in macrophages

Focusing on the r*Tc*-MUC-1–CFL1 and r*Tc*-MUC-1–FABP5 interactions, functional information on other proteins from murine macrophages initially identified in the pull-down assay were manually curated. CFL1 has a relatively complicated network with 17 of the identified proteins of RAW264.7 cells (S6 Table), including ARHGDIA and PFN1, which were not, or only weakly, identified using the co-immunoprecipitation (co-IP) assay. These molecules appear to dominate functionally in cell activation (e.g. cellular response to stimulus) and actin filament-based processes (e.g. extracellular matrix organization, cell migration and adhesion), and in actin-based cytoskeletal dynamics regulation-associated signalling (S7 and S8 Tables). Although no protein association network was predicted for FABP5 (S6 Table), this fatty acid-binding protein as well as malic enzyme 1 (ME1) and ubiquitin C (UBC) were predicted to be involved in the peroxisome proliferator-activated receptor (PPAR) signalling pathway (S8 Table). An integration of the biological information for CFL1, FABP5 and associated proteins indicates roles for *Tc*-MUC-1 in regulating the cytoskeletal dynamics and adipocytokine signalling of murine macrophages, particularly in the positive regulation of extracellular matrix organization (Fig 5).

Tc-MUC-1 without signal peptide		CFL1
Ionic interaction	96Asp	32Arg
Hydrogen bond	116Arg	32Arg
Cation-Pi interaction	100Phe	23/24Ser

Tc-MUC-1 without signal peptide		FABP5
Ionic interaction	150Arg	71Glu
Hydrogen bond	105Phe	50Asn
	150Arg	70Glu

Fig 4. *In silico* docking of *Toxocara canis* mucin 1 (*Tc*-MUC-1) protein and two key interacting proteins. (**A**) Protein complex predicted for *Tc*-MUC-1 and the cofilin 1 (CFL1) of murine RAW264.7 macrophage cells. Structures of *Tc*-MUC-1 and CFL1 are indicated in grey and red, respectively. (**B**) Protein complex predicted for *Tc*-MUC-1 and a dimer of the fatty acid binding protein 5 (FABP5) of murine RAW264.7 macrophages. Structures of *Tc*-MUC-1 and FABP5 are indicated in grey and red, respectively. Ionic interactions, hydrogen bonds or cation-pi binding interaction between the residues in *Tc*-MUC-1 (grey) and CFL1 (red) are indicated.

https://doi.org/10.1371/journal.pntd.0010734.g004
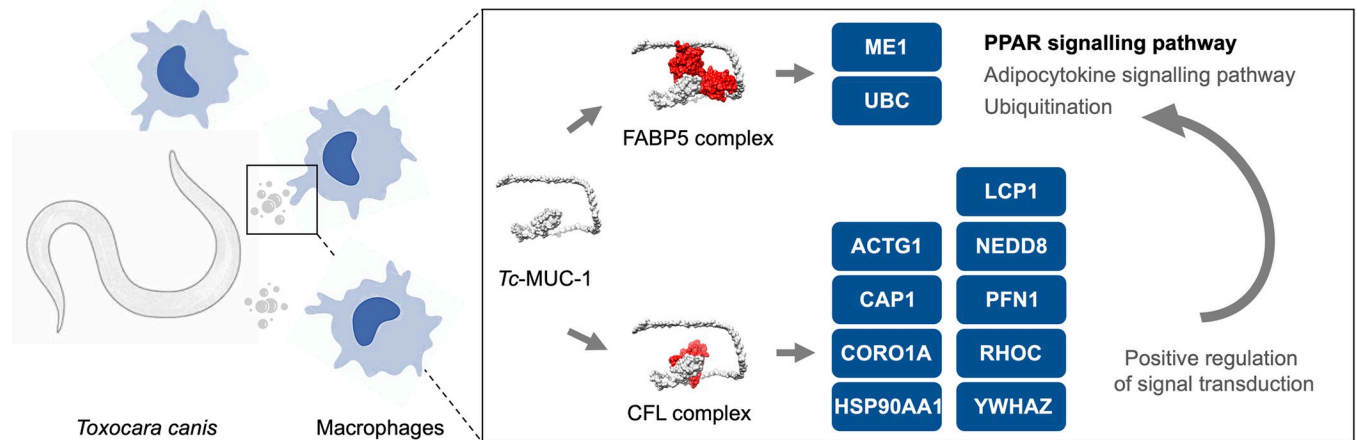
Fig 5. Schematic diagram summarising the inferred functions of cofilin 1 (CFL1) and fatty acid binding protein 5 (FABP5) that interact with a prokaryotically-expressed (non-glycosylated) recombinant form of the *Toxocara canis* mucin 1 protein (r*Tc*-MUC-1). FABP5 and CFL1 physically interact with r*Tc*-MUC-1, and are inferred to positively regulate cellular processes. FABP5 transports fatty acid ligands to activate peroxisome proliferator-activated receptors (PPAR), which then regulate the transcription of genes coding for malic enzyme 1 (ME1) and for ubiquitin C (UBC), participating in adipocytokine signalling pathway associated lipogenesis and ubiquitination, respectively. CFL interacts with actin gamma 1 (ACTG1), cyclase associated actin cytoskeleton regulatory protein 1 (CAP1), coronin actin binding protein 1A (CORO1A), heat shock protein 90 alpha family class A member 1 (HSP90AA1), lymphocyte cytosolic protein 1 (LCP1), ubiquitin-like modifier (NEDD8), PFN1, Ras homologue family member C (RHOC) and 14-3-3 protein zeta (YWHAZ), to positively regulate ME1-associated signal transduction in the adipocytokine signalling pathway.

Discussion

Using an integrated pull-down, mass spectrometry, co-IP and bioinformatic approach, we investigated the interactions between the non-glycosylated form of the *Tc*-MUC-1 protein and macrophages of the murine host; r*Tc*-MUC-1 was shown to be physically interactive with CFL1 and FABP5 from murine RAW264.7 macrophage cells. The integration of information from the protein association networks/pathways for the two proteins suggested that the *Tc*-MUC-1 protein plays a role in interfering cytoskeletal organisation and signal transduction in host macrophages.

The surface coat glycoprotein MUC-1 of *T. canis* has a protein binding activity. In the 1990s, it was shown that the mucin- and glycan-rich assembly form the "fuzzy coat" of *T. canis*, which appears to play a key role in shedding the surface coat with bound immune cells [20,45,46]. To date, a family of secreted mucins, namely MUC-1, -2, -3, -4 and -5, has been identified in the infective larvae of *T. canis* [47,48]. The proteins of each of these molecules are "hybrids", being unique among mucins in having acquired two ShKT domains [47,48]. One possibility is that this acquisition has conferred new properties, such as the interaction with proteins of host immune cells that promote infection. Although the ShKT domain is found in the potassium channel inhibitor ShK (a toxin) in sea anemone [49], it has been proposed to bind molecules without exhibiting a toxic effect [47]. Indeed, by performing His pull-down and co-IP assays, we confirmed that r*Tc*-MUC-1 did bind to the actin binding protein CFL1 of macrophages and a fatty acid binding protein FABP5 of the RAW264.7 cell line. The *Tc*-MUC-1–CFL1 and *Tc*-MUC-1–FABP5 complexes were modelled *in silico*, and strong hydrogen bonds were predicted, supporting previous speculation that the formation of intermolecular complexes with the ShK/SXC domains might be through non-covalent means [47]. Crystal structures of these complexes should confirm the binding sites of the *Tc*-MUC-1 protein, although protein structures were modelled with the machine learning-based program Alpha-Fold2 [41]. N-glycosylation of *Tc*-MUC-1-FLAG in HEK 293T cells might explain why no interactions with AKR1B3, ARHGDIA, PFN1 or PRDX1 that were detected by pull-down

experiment. Future mutation experiments should define which key residues in r*Tc*-MUC-1 are directly involved in binding CFL1 and/or FABP5 of murine RAW264.7 macrophages.

By binding to the actin binding protein cofilin 1, the *Tc*-MUC-1 protein is likely to interfere with the migration and phagocytosis of macrophage cells. Like other pathogen molecules detected by host animals, the mucins of parasites can be recognised by innate immune cells [20,50]. It is well known that the specialised monocytes (e.g. macrophages) play essential roles in the detection and elimination of pathogens, including parasitic worms [51–53]. In this process, cell migration and phagocytosis are involved, which rely on a dynamic remodelling of actin cytoskeleton. Cofilin is one of the actin-binding proteins demonstrated to play roles in the actin cytoskeletal remodelling, migration directionality and phagosome formation of macrophages [54,55]. Interestingly, in the current study, we showed that the r*Tc*-MUC-1 interacts with the actin binding protein CFL1 of the macrophage-like Abelson leukaemia virus-transformed cell line derived from BALB/c mice (RAW264.7) that has been commonly used to explore parasite-host interactions [56–58]. CFL1 was also predicted to associate with other proteins that were identified in the pull-down assay, including actin, cyclase associated actin cytoskeleton regulatory protein, coronin actin binding protein, lymphocyte cytosolic protein and Rho GDP dissociation inhibitor alpha, which are known to play roles in the myosin contraction and cofilin-mediated disassembly during macrophage migration [54,55]. These results strongly suggest that the *Tc*-MUC-1 protein, by interacting with CFL1, affects the migration and phagosome formation of host macrophages in innate immune responses.

The *Tc*-MUC-1 protein might also play a role in regulating the signal transduction in host immune cells. This statement could be supported by an association network of CFL1 with the identified signalling molecules involved in cell shape, attachment and motility, including Rho GTPases and 14-3-3 protein zeta [59–61]. Therefore, by interacting with CFL1, the *Tc*-MUC-1 protein is likely to influence the cell locomotion of stimulated macrophages; this protein might also play a role in modulating inflammation-associated signalling pathways, as interacting molecules (i.e. fatty acid binding protein 5 and the associated NADP-dependent enzyme ME1 and polyubiquitin precursor UBC) are known to transfer specific fatty acids from the cytosol to the nucleus, wherein they activate nuclear receptors linked to the modulation of NF-kappa-B signalling during inflammation [62,63]. Indeed, mucins of *T. canis* have been reported to play roles in the stimulation of immune cells of host animals, particularly via IL-10 and proinflammation cytokine production and Toll-like receptor signalling *in vitro* [23,24]. Further studies should explore the regulatory role(s) of *Tc*-MUC-1 on immune recognition and/or evasion (e.g., *via* macrophage proliferation/activation, expression of major histocompatibility complex (MHC) class II molecules, cytokine secretion and/or calcium flux).

Questions surrounding *Toxocara* mucins that also warrant investigation in the future include: Do sugar moieties of *Tc*-MUC-1 have an impact on its recognition by host macrophage cells?–as it has been reported that such elements are important in antibody-mediated immune responses [27]. Do the ShKT domains of the *Tc*-MUC-1 protein play roles in altering innate immune responses of host animals?–as ShKT domain-containing peroxidase and associated cuticle development of *C. elegans* has been reported to be involved in pathogen resistance [64–66]. Are mucins involved in the tuft cell activation?–which has been emerging a novel aspect for understanding intestinal immune responses to parasitic infections [67]. Addressing these questions should improve our understanding of the interplay between *T. canis* larvae and host cells.

In conclusion, we demonstrated that a non-glycosylated, recombinant form of the protein of *Tc*-MUC-1 interacts with the actin binding protein CFL1 and the fatty acid binding protein FABP5 of murine RAW264.7 macrophages *in vitro*. These findings suggest that the *Tc*-MUC-1 protein might interfere with the migration and phagocytosis of host macrophages, providing

new insight into the host-parasite interplay at the molecular and cellular levels. Further investigations of glycosylated *Tc*-MUC-1 in the interaction with host (murine and human) macrophages, and other species of *Toxocara* and ascaridoids should establish whether immune recognition and modulation are genus- or species-specific.

Supporting information

S1 Table. Oligonucleotide primer sets used for the PCR-based amplification of coding sequences for subsequent protein expression in HEK 293T cells.
(XLSX)

S2 Table. Peptides of proteins of RAW264.7 cells identified to interact with the r*Tc*-MUC-1 protein by His pull-down and LC-MS/MS.
(XLSX)

S3 Table. Proteins of RAW264.7 cells identified to interact with the r*Tc*-MUC-1 protein by His pull-down and LC-MS/MS.
(XLSX)

S4 Table. Gene Ontology (GO) annotation of proteins of RAW264.7 cells identified to interact with the r*Tc*-MUC-1 protein.
(XLSX)

S5 Table. Kyoto Encyclopedia of Genes and Genomes (KEGG) annotation of proteins of RAW264.7 cells identified to interact with the r*Tc*-MUC-1 protein.
(XLSX)

S6 Table. Networks of proteins of RAW264.7 cells identified to interact with the r*Tc*-MUC-1 protein.
(XLSX)

S7 Table. Biological process annotations for proteins of RAW264.7 cells identified to interact with CFL1 and FABP5.
(XLSX)

S8 Table. Pathway annotations of proteins of RAW264.7 cells identified to interact with CFL1 and FABP5.
(XLSX)

S1 Fig. Gene Ontology (GO) annotation of proteins of RAW264.7 cells identified to interact with the r*Tc*-MUC-1 protein. Enrichment analyses of proteins bound to recombinant *Toxocara canis* mucin 1 (r*Tc*-MUC-1) for (**A**) cellular component, (**B**) molecular function, and (**C**) biological process. Predominant annotation enrichments and the percentages are underlined.
(TIF)

S2 Fig. Pathway enrichment for proteins of RAW264.7 cells identified to interact with the r*Tc*-MUC-1 protein.
(TIF)

S3 Fig. Protein association network predicted for the proteins identified in RAW264.7 cells.
(TIF)

S4 Fig. Western blot analyses of the expression of HA-tagged proteins of RAW264.3 and FLAG-tagged *Tc*-MUC-1 in transfected HEK 293T cells. Lanes 1–7: PRDX1, PFN1, CFL1, AKR1B3, FABP5, ARHGDIA and FLAG-tagged *Tc*-MUC-1. M: Maker.
(TIF)

Acknowledgments

Author Contributions

Conceptualization: Rongqiong Zhou, Robin B. Gasser, Guangxu Ma.

Data curation: Rongqiong Zhou, Hongguo Jia, Zhendong Du, Aiyun Jiang, Zhenhui Song, Tao Wang.

Formal analysis: Hongguo Jia, Zhendong Du, Aiyun Jiang, Guangxu Ma.

Funding acquisition: Rongqiong Zhou, Robin B. Gasser, Guangxu Ma.

Investigation: Hongguo Jia, Aiyun Jiang, Zhenhui Song.

Project administration: Rongqiong Zhou.

Software: Zhendong Du.

Supervision: Rongqiong Zhou, Robin B. Gasser, Guangxu Ma.

Validation: Tao Wang, Aifang Du.

Visualization: Zhendong Du.

Writing – original draft: Rongqiong Zhou, Guangxu Ma.

Writing – review & editing: Aifang Du, Robin B. Gasser, Guangxu Ma.

References

1. Ma G, Holland CV, Wang T, Hofmann A, Fan C-K, Maizels RM, et al. Human toxocariasis. Lancet Infect Dis. 2018; 18: e14–e24. https://doi.org/10.1016/S1473-3099(17)30331-6 PMID: 28781085

2. Strube C, Heuer L, Janecek E. *Toxocara* spp. infections in paratenic hosts. Vet Parasitol. 2013; 193: 375–89. https://doi.org/10.1016/j.vetpar.2012.12.033 PMID: 23312872

3. Fisher M. *Toxocara cati*: an underestimated zoonotic agent. Trends Parasitol. 2003; 19: 167–70. https://doi.org/10.1016/s1471-4922(03)00027-8

4. Rostami A, Riahi SM, Holland CV, Taghipour A, Khalili-Fomeshi M, Fakhri Y, et al. Seroprevalence estimates for toxocariasis in people worldwide: A systematic review and meta-analysis. PLoS Negl Trop Dis. 2019; 13: e0007809. https://doi.org/10.1371/journal.pntd.0007809 PMID: 31856156

5. Ma G, Rostami A, Wang T, Hofmann A, Hotez PJ, Gasser RB. Global and regional seroprevalence estimates for human toxocariasis: A call for action. Adv Parasitol. 2020; 109: 275–90. https://doi.org/10.1016/bs.apar.2020.01.011 PMID: 32381202

6. Mohammadzadeh I, Riahi SM, Saber V, Darvish S, Amrovani M, Arefkhah N, et al. The relationship between *Toxocara* species seropositivity and allergic skin disorders: a systematic review and meta-analysis. Trans R Soc Trop Med Hyg. 2018; 112: 529–37. https://doi.org/10.1093/trstmh/try094 PMID: 30184239

7. Aghaei S, Riahi SM, Rostami A, Mohammadzadeh I, Javanian M, Tohidi E, et al. *Toxocara* spp. infection and risk of childhood asthma: A systematic review and meta-analysis. Acta Trop. 2018; 182: 298–304. https://doi.org/10.1016/j.actatropica.2018.03.022 PMID: 29573999

8. Fan C-K, Holland CV, Loxton K, Barghouth U. Cerebral toxocariasis: Silent progression to neurodegenerative disorders? Clin Microbiol Rev. 2015; 28: 663–86. https://doi.org/10.1128/CMR.00106-14 PMID: 26062575

9. Cooper PJ. *Toxocara canis* infection: an important and neglected environmental risk factor for asthma? Clin Exp Allergy. 2008; 38: 551–3. https://doi.org/10.1111/j.1365-2222.2008.02934.x PMID: 18241245

10. Li L, Gao W, Yang X, Wu D, Bi H, Zhang S, et al. Asthma and toxocariasis. Ann Allergy Asthma Immunol. 2014; 113: 187–92. https://doi.org/10.1016/j.anai.2014.05.016 PMID: 24934109

11. Fan C-K. Pathogenesis of cerebral toxocariasis and neurodegenerative diseases. Adv Parasitol. 2020; 109: 233–59. https://doi.org/10.1016/bs.apar.2020.01.008 PMID: 32381200

12. Strube C, Waindok P, Raulf M-K, Springer A. *Toxocara*-induced neural larva migrans (neurotoxocarosis) in rodent model hosts. Adv Parasitol. 2020; 109: 189–218. https://doi.org/10.1016/bs.apar.2020.01.006 PMID: 32381198

13. Holland CV, Cox DM. *Toxocara* in the mouse: a model for parasite-altered host behaviour? J Helminthol. 2001; 75: 125–35. https://doi.org/10.1079/joh200169

14. Bowman DD. *Toxocara* and Toxocariasis. 1 st ed. London: Elsevier Science; 2020.

15. Nichols RL. The etiology of visceral larva migrans: I. diagnostic morphology of infective second-stage *Toxocara* larvae. J Parasitol. 1956; 42: 349. https://doi.org/10.2307/3274518

16. Wilder HC. Nematode endophthalmitis. Trans Am Acad Ophthalmol Otolaryngol. 1950; 55: 99–109. PMID: 14798648

17. Holland CV, Smith HV. *Toxocara*: The Enigmatic Parasite. 1 st ed. Oxfordshire: CABI; 2006. https://doi.org/10.1079/9781845930264.0000

18. Gasser RB, Korhonen PK, Zhu X-Q, Young ND. Harnessing the *Toxocara* genome to underpin toxocariasis research and new interventions. Adv Parasitol. 2016; 91: 87–110. https://doi.org/10.1016/bs.apar.2015.12.001 PMID: 27015948

19. Zheng W-B, Zou Y, Zhu X-Q, Liu G-H. *Toxocara* "omics" and the promises it holds for medicine and veterinary medicine. Adv Parasitol. 2020; 109: 89–108. https://doi.org/10.1016/bs.apar.2020.01.002 PMID: 32381233

20. Maizels RM. *Toxocara canis*: Molecular basis of immune recognition and evasion. Vet Parasitol. 2013; 193: 365–74. https://doi.org/10.1016/j.vetpar.2012.12.032 PMID: 23351972

21. Maizels RM, Tetteh KK, Loukas A. *Toxocara canis*: genes expressed by the arrested infective larval stage of a parasitic nematode. Int J Parasitol. 2000; 30: 495–508. https://doi.org/10.1016/s0020-7519(00)00022-9

22. Li F, Li XL, Chen SJ, Tan C, Mei SP, Jia HG, et al. Excretory/secretory proteins of adult *Toxocara canis* induce changes in the expression of proteins involved in the NOD1-RIP2-NF-κB pathway and modulate cytokine production in mouse macrophages. Exp Parasitol. 2021; 229: 108152. https://doi.org/10.1016/j.exppara.2021.108152 PMID: 34419413

23. Długosz E, Wasyl K, Klockiewicz M, Wiśniewski M. *Toxocara canis* mucins among other excretory-secretory antigens induce *in vitro* secretion of cytokines by mouse splenocytes. Parasitol Res. 2015; 114: 3365–71. https://doi.org/10.1007/s00436-015-4561-5 PMID: 26044883

24. Długosz E, Basałaj K, Zawistowska-Deniziak A. Cytokine production and signalling in human THP-1 macrophages is dependent on *Toxocara canis* glycans. Parasitol Res. 2019; 118: 2925–33. https://doi.org/10.1007/s00436-019-06405-8 PMID: 31396715

25. Fong M-Y, Lau Y-L. Recombinant expression of the larval excretory-secretory antigen TES-120 of *Toxocara canis* in the methylotrophic yeast *Pichia pastoris*. Parasitol Res. 2004; 92: 173–6. https://doi.org/10.1007/s00436-003-1020-5 PMID: 14655048

26. Fong M-Y, Lau Y-L, Init I, Jamaiah I, Anuar AK, Rahmah N. Recombinant expression of *Toxocara canis* excretory-secretory antigen TES-120 in *Escherichia coli*. Southeast Asian J Trop Med Public Health. 2003; 34: 723–6.

27. Długosz E, Wiśniewski M. *Toxocara canis* glycans influence antigen recognition by mouse IgG1 and IgM antibodies. Acta Parasitol. 2016; 61: 191–4. https://doi.org/10.1515/ap-2016-0026 PMID: 26751891

28. Holland CV, Hamilton CM. The significance of cerebral toxocariasis: a model system for exploring the link between brain involvement, behaviour and the immune response. J Exp Biol. 2013; 216: 78–83. https://doi.org/10.1242/jeb.074120 PMID: 23225870

29. Mehlhorn H. Baermann's larval technique. In: Mehlhorn H, editor. Encyclopedia of Parasitology. 1 st ed. Berlin, Germany: Springer; 2016.

30. Gems D, Maizels RM. An abundantly expressed mucin-like protein from *Toxocara canis* infective larvae: the precursor of the larval surface coat glycoproteins. Proc Natl Acad Sci U S A. 1996; 93: 1665–70. https://doi.org/10.1073/pnas.93.4.1665 PMID: 8643687

31. Finn RD, Clements J, Eddy SR. HMMER web server: interactive sequence similarity searching. Nucleic Acids Res. 2011; 39: W29–37. https://doi.org/10.1093/nar/gkr367 PMID: 21593126

32. Ma GX, Zhou RQ, Huang HC, Hu SJ, Lin J. Tissue-specific distribution of serine/threonine protein phosphatase 1 of *Toxocara canis*. Vet Parasitol. 2014; 205: 551–7. https://doi.org/10.1016/j.vetpar.2014.09.010 PMID: 25282049

33. Green MR, Sambrook J. Molecular Cloning: A Laboratory Manual. 4th ed. Cold Spring Harbor Laboratory Press; 2012.

34. Perez-Riverol Y, Csordas A, Bai J, Bernal-Llinares M, Hewapathirana S, Kundu DJ, et al. The PRIDE database and related tools and resources in 2019: improving support for quantification data. Nucleic Acids Res. 2019; 47: D442–50. https://doi.org/10.1093/nar/gky1106 PMID: 30395289

35. Bu D, Luo H, Huo P, Wang Z, Zhang S, He Z, et al. KOBAS-i: intelligent prioritization and exploratory visualization of biological functions for gene enrichment analysis. Nucleic Acids Res. 2021; 49: W317–25. https://doi.org/10.1093/nar/gkab447 PMID: 34086934

36. Szklarczyk D, Franceschini A, Wyder S, Forslund K, Heller D, Huerta-Cepas J, et al. STRING v10: protein–protein interaction networks, integrated over the tree of life. Nucleic Acids Res. 2015; 43: D447–52. https://doi.org/10.1093/nar/gku1003 PMID: 25352553

37. Shannon P, Markiel A, Ozier O, Baliga NS, Wang JT, Ramage D, et al. Cytoscape: a software environment for integrated models of biomolecular interaction networks. Genome Res. 2003; 13: 2498–504. https://doi.org/10.1101/gr.1239303 PMID: 14597658

38. Roy A, Kucukural A, Zhang Y. I-TASSER: a unified platform for automated protein structure and function prediction. Nat Protoc. 2010; 5: 725–38. https://doi.org/10.1038/nprot.2010.5 PMID: 20360767

39. Zhang Y. I-TASSER server for protein 3D structure prediction. BMC Bioinformatics. 2008; 9: 40. https://doi.org/10.1186/1471-2105-9-40 PMID: 18215316

40. Yang J, Yan R, Roy A, Xu D, Poisson J, Zhang Y. The I-TASSER Suite: protein structure and function prediction. Nat Methods. 2015; 12: 7–8. https://doi.org/10.1038/nmeth.3213 PMID: 25549265

41. Jumper J, Evans R, Pritzel A, Green T, Figurnov M, Ronneberger O, et al. Highly accurate protein structure prediction with AlphaFold. Nature. 2021; 596: 583–9. https://doi.org/10.1038/s41586-021-03819-2 PMID: 34265844

42. Comeau SR, Gatchell DW, Vajda S, Camacho CJ. ClusPro: a fully automated algorithm for protein–protein docking. Nucleic Acids Res. 2004; 32: W96–9. https://doi.org/10.1093/nar/gkh354 PMID: 15215358

43. Kozakov D, Hall DR, Xia B, Porter KA, Padhorny D, Yueh C, et al. The ClusPro web server for protein–protein docking. Nat Protoc. 2017; 12: 255–78. https://doi.org/10.1038/nprot.2016.169 PMID: 28079879

44. Sanson B, Wang T, Sun J, Wang L, Kaczocha M, Ojima I, et al. Crystallographic study of FABP5 as an intracellular endocannabinoid transporter. Acta Crystallogr D Biol Crystallogr. 2014; 70: 290–8. https://doi.org/10.1107/S1399004713026795 PMID: 24531463

45. Fattah DI, Maizels RM, McLaren DJ, Spry CJ. *Toxocara canis*: Interaction of human blood eosinophils with the infective larvae. Exp Parasitol. 1986; 61: 421–31. https://doi.org/10.1016/0014-4894(86)90198-0

46. Badley JE, Grieve RB, Rockey JH, Glickman LT. Immune-mediated adherence of eosinophils to *Toxocara canis* infective larvae: the role of excretory-secretory antigens. Parasite Immunol. 1987; 9: 133–43. https://doi.org/10.1111/j.1365-3024.1987.tb00494.x

47. Loukas A, Hintz M, Linder D, Mullin NP, Parkinson J, Tetteh KK, et al. A family of secreted mucins from the parasitic nematode *Toxocara canis* bears diverse mucin domains but shares similar flanking six-cysteine repeat motifs*. J Biol Chem. 2000; 275: 39600–07. https://doi.org/10.1074/jbc.m005632200 PMID: 10950959

48. Doedens A, Loukas A, Maizels RM. A cDNA encoding *Tc*-MUC-5, a mucin from *Toxocara canis* larvae identified by expression screening. Acta Trop. 2001; 79: 211–7. https://doi.org/10.1016/s0001-706x(01)00137-1

49. Dauplais M, Lecoq A, Song J, Cotton J, Jamin N, Gilquin B, et al. On the convergent evolution of animal toxins conservation of a diad of functional residues in potassium channel-blocking toxins with unrelated structures*. J Biol Chem. 1997; 272: 4302–9. https://doi.org/10.1074/jbc.272.7.4302 PMID: 9020148

50. Raulf M-K, Lepenies B, Strube C. *Toxocara canis* and *Toxocara cati* somatic and excretory-secretory antigens are recognised by C-type lectin receptors. Pathogens. 2021; 10: 321. https://doi.org/10.3390/pathogens10030321 PMID: 33803269

51. Viney M. How do host immune responses affect nematode infections? Trends Parasitol. 2002; 18: 63–6. https://doi.org/10.1016/s1471-4922(01)02171-7 PMID: 11832295

52. Allen JE, Maizels RM. Diversity and dialogue in immunity to helminths. Nat Rev Immunol. 2011; 11: 375–88. https://doi.org/10.1038/nri2992 PMID: 21610741

53. Webb LM, Wojno EDT. The role of rare innate immune cells in Type 2 immune activation against parasitic helminths. Parasitology. 2017; 144: 1–14. https://doi.org/10.1017/s0031182017000488 PMID: 28583216

54. Yolland L, Burki M, Marcotti S, Luchici A, Kenny FN, Davis JR, et al. Persistent and polarized global actin flow is essential for directionality during cell migration. Nat Cell Biol. 2019; 21: 1370–81. https://doi.org/10.1038/s41556-019-0411-5 PMID: 31685997

55. Lu Y, Cao L, Egami Y, Kawai K, Araki N. Cofilin contributes to phagocytosis of IgG-opsonized particles but not non-opsonized particles in RAW264 macrophages. Microscopy (Oxf). 2016; 65: 233–42. https://doi.org/10.1093/jmicro/dfv376 PMID: 26754560

56. Zheng Y, Guo X, Su M, Guo A, Ding J, Yang J, et al. Regulatory effects of *Echinococcus multilocularis* extracellular vesicles on RAW264.7 macrophages. Vet Parasitol. 2017; 235: 29–36. https://doi.org/10.1016/j.vetpar.2017.01.012 PMID: 28215864

57. Nadaes NR, Costa LS da, Santana RC, LaRocque-de-Freitas IF, Vivarini Á de C, Soares DC, et al. DH82 canine and RAW264.7 murine macrophage cell lines display distinct activation profiles upon interaction with *Leishmania infantum* and *Leishmania amazonensis*. Front Cell Infect Microbiol. 2020; 10: 247. https://doi.org/10.3389/fcimb.2020.00247 PMID: 32596164

58. Wang Z, Hao C, Zhuang Q, Zhan B, Sun X, Huang J, et al. Excretory/secretory products from *Trichinella spiralis* adult worms attenuated DSS-induced colitis in mice by driving PD-1-mediated M2 macrophage polarization. Front Immunol. 2020; 11: 563784. https://doi.org/10.3389/fimmu.2020.563784 PMID: 33117347

59. Ridley AJ, Schwartz MA, Burridge K, Firtel RA, Ginsberg MH, Borisy G, et al. Cell migration: integrating signals from front to back. Science. 2003; 302: 1704–9. https://doi.org/10.1126/science.1092053 PMID: 14657486

60. Etienne-Manneville S, Hall A. Rho GTPases in cell biology. Nature. 2002; 420: 629–35. https://doi.org/10.1038/nature01148 PMID: 12478284

61. Hubel P, Urban C, Bergant V, Schneider WM, Knauer B, Stukalov A, et al. A protein-interaction network of interferon-stimulated genes extends the innate immune system landscape. Nat Immunol. 2019; 20: 493–502. https://doi.org/10.1038/s41590-019-0323-3 PMID: 30833792

62. Armstrong EH, Goswami D, Griffin PR, Noy N, Ortlund EA. Structural basis for ligand regulation of the fatty acid-binding protein 5, peroxisome proliferator-activated receptor β/δ (FABP5-PPARβ/δ) signaling pathway*. J Biol Chem. 2014; 289: 14941–54. https://doi.org/10.1074/jbc.M113.514646 PMID: 24692551

63. Sheng C, Yao C, Wang Z, Chen H, Zhao Y, Xu D, et al. Cyclophilin J limits inflammation through the blockage of ubiquitin chain sensing. Nat Commun. 2018; 9: 4381. https://doi.org/10.1038/s41467-018-06756-3 PMID: 30348973

64. Tiller GR, Garsin DA. The SKPO-1 peroxidase functions in the hypodermis to protect *Caenorhabditis elegans* from bacterial infection. Genetics. 2014; 197: 515–26. https://doi.org/10.1534/genetics.113.160606 PMID: 24621828

65. Liu Y, Kaval KG, Hoof A van, Garsin DA. Heme peroxidase HPX-2 protects *Caenorhabditis elegans* from pathogens. PLoS Genet. 2019; 15: e1007944. https://doi.org/10.1371/journal.pgen.1007944 PMID: 30695063

66. Liu Y, Martinez-Martinez D, Essmann CL, Cruz MR, Cabreiro F, Garsin DA. Transcriptome analysis of *Caenorhabditis elegans* lacking heme peroxidase SKPO-1 reveals an altered response to *Enterococcus faecalis*. G3 (Bethesda). 2020; 11: jkaa055. https://doi.org/10.1093/g3journal/jkaa055 PMID: 33609366

67. Gerbe F, Sidot E, Smyth DJ, Ohmoto M, Matsumoto I, Dardalhon V, et al. Intestinal epithelial tuft cells initiate type 2 mucosal immunity to helminth parasites. Nature. 2016; 529: 226–30. https://doi.org/10.1038/nature16527 PMID: 26762460